Light: Science & Applications (2014) 3, e129; doi:10.1038/lsa.2014.10
© 2014 CIOMP. All rights reserved 2047-7538/14
www.nature.com/lsa

ORIGINAL ARTICLE

Protein-based soft micro-optics fabricated by femtosecond laser direct writing

Yun-Lu Sun[1], Wen-Fei Dong[1], Li-Gang Niu[1], Tong Jiang[1], Dong-Xu Liu[1], Lu Zhang[1], Ying-Shuai Wang[1], Qi-Dai Chen[1], Dong-Pyo Kim[3] and Hong-Bo Sun[1,2]

In this work, we report a novel soft diffractive micro-optics, called 'microscale kinoform phase-type lens (micro-KPL)', which is fabricated by femtosecond laser direct writing (FsLDW) using bovine serum albumin (BSA) as building blocks and flexible polydimethylsiloxane (PDMS) slices as substrates. By carefully optimizing various process parameters of FsLDW (e.g., average laser power density, scanning step, exposure time on a single point and protein concentration), the as-formed protein micro-KPLs exhibit excellent surface quality, well-defined three-dimensional (3D) geometry and distinctive optical properties, even in relatively harsh operation environments (for instance, in strong acid or base). Laser shaping, imaging and other optical performances can be easily achieved. More importantly, micro-KPLs also have unique flexible and stretchable properties as well as good biocompatibility and biodegradability. Therefore, such protein hydrogel-based micro-optics may have great potential applications, such as in flexible and stretchable photonics and optics, soft integrated optical microsystems and bioimplantable devices.
Light: Science & Applications (2014) **3,** e129; doi:10.1038/lsa.2014.10; published online 17 January 2014

Keywords: femtosecond laser direct writing; micro-optics; protein; soft

INTRODUCTION

Soft micro-optics, which can be twisted, folded, compressed and stretched repeatedly without any significant damage to mechanical or optical characteristics, have become increasingly important in applications such as adaptive microlenses,[1] paper-like displays,[2,3] solar cells,[4–6] photonic integrated systems[7,8] and, most notably, bio-integrated and bio-implantable photonic micro/nanodevices.[9–17] Until now, numerous fabrication methods, for instance, transferring-and-printing processes, hot-embossing technique, nano-imprinting, and self-assembly approaches, have been developed to produce flexible and stretchable micro-optics using organic, polymer, silk or hydrogel materials.[13–20] Owing to their abundance, renewability, inexpensiveness, degradability, biocompatibility and unique functionality, protein-based soft micro-optics demonstrate superior performances that exceed many devices made from currently available organic materials. However, developing a convenient, economic and ecofriendly fabrication strategy that could readily produce high-performance protein-based soft micro-optics with high accuracy and improved quality is challenging. Toward this end, the novel femtosecond laser direct writing (FsLDW) method offers compelling advantages; it is a facile, rapid, non-contact and maskless approach that can realize arbitrary, designable and complicated architectures with a nanometric resolution, which conventional methods fail to provide.[21–24]

Recently, it has been demonstrated that biocompatible protein micro/nanoscale structures and devices (e.g., micro-optics) could be successfully fabricated by FsLDW techniques.[25–31] Due to the low collateral damage of FsLDW, which achieved by high spacial restriction of the laser energy and a Fs-scale pulse width that is much shorter than the thermal diffusion time, these protein microstructures exhibit unique bioactivities,[25] good biocompatibility and good tunability under appropriate external stimuli.[26,27] However, the quality of protein micro-optics has been highly improved by optimized laser processing and the self-smoothing effect after two-photon-induced polymerization, which ensures their high performance optical properties.[26,27] Despite the significant progress that has been achieved to date, the existing protein micro-optics have not taken full advantage of their soft features (both flexibility and stretchability) and have not been applied as soft micro-optics, which ultimately limits their further applications. For this reason, in this work, we will report a soft diffractive micro-optics, called 'microscale kinoform phase-type lenses (micro-KPL)', fabricated by FsLDW using bovine serum albumin (BSA) as building blocks and flexible polydimethylsiloxane (PDMS) slices as substrates. The protein soft micro-optics exhibit not only unique flexible and stretchable properties, but also good biocompatibility and biodegradability. Furthermore, the long-term stability of the optical profile and surface morphology of micro-KPLs can be

[1]State Key Laboratory on Integrated Optoelectronics, College of Electronic Science and Engineering, Jilin University, Changchun 130012, China; [2]College of Physics, Jilin University, Changchun 130023, China and [3]National Center of Applied Microfluidic Chemistry, Department of Chemical Engineering, Pohang University of Science and Technology, Pohang 790-784, Korea
Correspondence: Professor WF Dong, State Key Laboratory on Integrated Optoelectronics, College of Electronic Science and Engineering, Jilin University, 2699 Qianjin Street, Changchun 130012, China
E-mail: wenfeidong@126.com
Or Professor HB Sun, State Key Laboratory on Integrated Optoelectronics, College of Electronic Science and Engineering, Jilin University, 2699 Qianjin Street, Changchun 130012, China
E-mail: hbsun@jlu.edu.cn
Received 1 May 2013; revised 5 September 2013; accepted 16 September 2013

demonstrated in air, pure water and even a strong acid or base solution. All of these merits give the protein micro-KPLs great potential for practical applications as an environment-friendly soft micro-optics.

MATERIALS AND METHODS

Preparation of the protein aqueous ink for FsLDW

Appropriate amounts of BSA (product no. A7638; Sigma-Aldrich) and methylene blue (product no. M9140; Aldrich, Sigma-Aldrich, Co. 3050 Spruce Street, St. Louis. MO 63103 USA.) were dissolved in phosphate buffer (pH=7.4) to obtain a protein aqueous ink containing 600 mg mL^{-1} BSA and 0.6 mg mL^{-1} methylene blue. The solution needed to be incubated for several hours at 4 ℃ for sufficient dissolution of reagents. Ultrapure water (18.2 MΩ cm, 25 ℃), obtained using a MILLIPORE water purification system, was used in the experiment.

Preparation of buffers with different pH values

First, 0.71 g of NaH_2PO_4 (Mr=142) and 2.181 g of NaCl were dissolved in approximately 450 mL of ultrapure water. Then, the solution was titrated to pH 7.41, as assessed by a pH meter (PB-21; Sartorius, Sartoriu AG, Weender Landstr. 94-108 37075 Goettingen, Germany), with a high-concentration NaOH aqueous solution. In addition, the volume was increased to 500 mL with ultrapure water. All the procedures were conducted at room temperature (~22 ℃). Thus, in the end, the buffer had a pH value of 7.40, and the ionic strength was 0.1 M at room temperature (~22 ℃). Phosphate buffers with ionic strength 0.1 M and pH values from 1.0 to 13.0 were obtained by similar procedures.

FsLDW of protein micro-KPLs

KPLs are high-efficiency phase-type diffractive lenses that consist concentrically of several odd and even zones.[32] In this work, protein micro-KPLs are composed of three odd and three even zones, as shown in Figure 1c and Figure 2a-1. The outer radius r_m of the mth zone (counting from the inside) of the protein micro-KPLs can be determined by the equation $r_m^2 + f^2 = (f + m\lambda/N)^2$, where f is the designed focal length, λ is the wavelength of light in vacuum and N is the level of micro-KPLs.[32] Here, $N=2^L$, where L is the number of layers of the micro-KPL. In this work, $L=1$ and $N=2$. Because $N=2$ and $m\lambda$ is much smaller than f, the formula can be rewritten as $f \approx r_m^2/m\lambda$. Thus, r_m and λ strongly affect f. Because f is inversely proportional to λ, KPL is a type of lens element with typical minus chromatic aberration. When light is passing through all zones, it will be interfered constructively at the focus due to the phase change induced by thickness variation. The maximum intensity is located at the focal spot. However, the diffraction efficiency of micro-KPLs is up to 40.5%, which is three times higher than that of Fresnel zone plates (amplitude-type diffractive lenses).[32] Because either the odd or the even zones of an Fresnel zone plate are opaque, much light is blocked. However, all the zones in the KPLs are transparent.[32] Due to the minus chromatic aberration profile and higher efficiency of diffractive microlenses, KPLs are widely used in applications such as laser shaping, imaging, and compact integrated optical systems.[32] Moreover, because a KPL's focal length is determined by $f \approx r_m^2/m\lambda$, r_m and λ are two main factors in determining f, and both parameters are stimuli-independent (for example, previous reports have shown that these parameters are not affected by pH-independent). These properties help to achieve a stimuli-independent protein microlens, which might be very useful in certain cases where stimuli-response is undesired (mainly bio-optical applications).

In our experiment, a homemade system for FsLDW was built to produce protein micro-KPLs. The aqueous mixture of BSA (600 mg mL^{-1}) and methylene blue (0.6 mg mL^{-1}), as a photosensitizer, was freshly prepared as the FsLDW ink prior to the laser fabrication. The

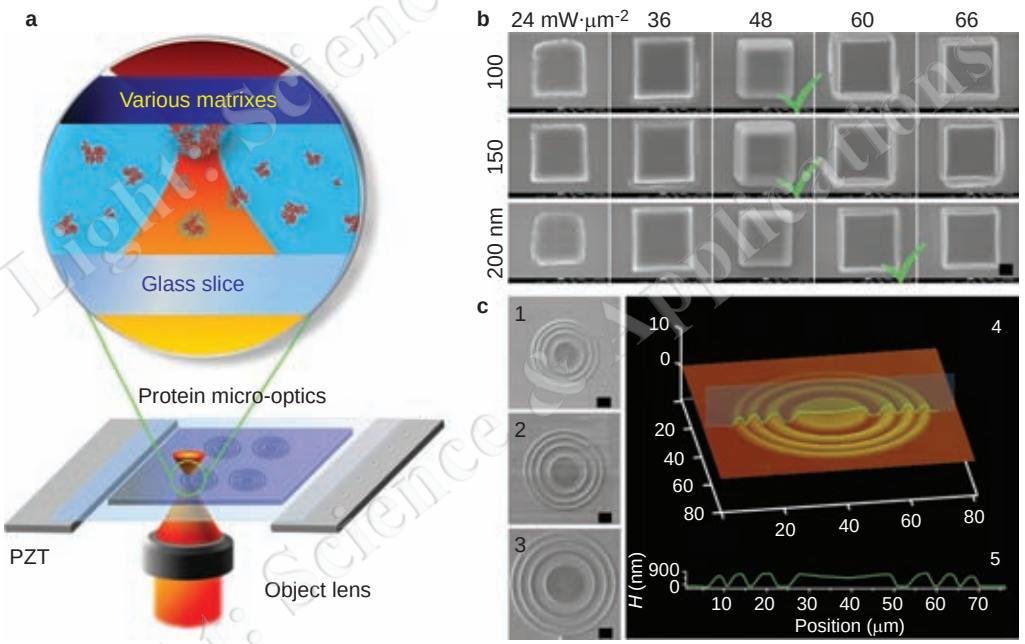

Figure 1 (**a**) Schematic of a homemade femtosecond laser 3D direct writing (FsLDW) approach and the preparation of a protein micro-optic. (**b**) SEM images (on a glass coverslip) showing topography influenced by average laser power density (measured before the objective, from ~24 mW μm^{-2} to ~66 mW μm^{-2}) and the scanning step (100 nm, 150 nm and 200 nm) when exposure time on single point is fixed at 1000 μs. The focal spot area where polymerization occurs is estimated to be ~0.40 μm^2. Scale bar=2 μm. (**c**) SEM images of protein micro-KPLs on a glass coverslip with thicknesses of ~1 μm but different diameters of (1) 50 μm, (2) 60 μm and (3) 80 μm. (4) AFM characterization exhibiting 3D morphology and ~10-nm average roughness of the protein micro-KPL (with a diameter of ~60 μm). The unit of the coordinates is μm. (5) The cross section at the central line of the protein micro-KPL in (4) by AFM. H stands for the thickness of the protein micro-KPL. Scale bar=10 μm. AFM, atomic force microscope; 3D, three-dimensional; FsLDW, femtosecond laser direct writing; micro-KPL, microscale kinoform phase-type lens; SEM, scanning electron microscopy.

doi:10.1038/lsa.2014.10

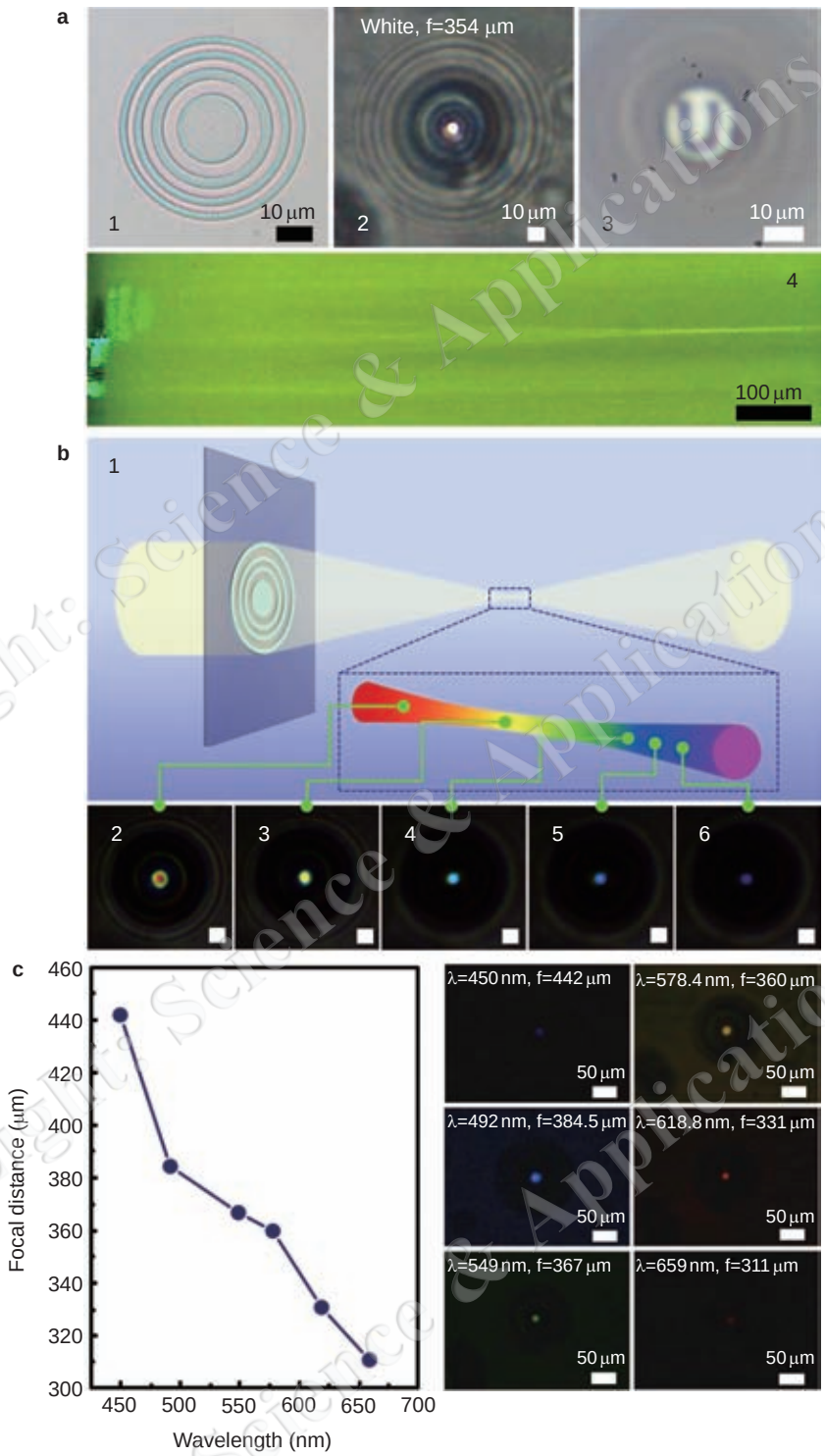

Figure 2 (**a-1**) The protein micro-KPL with a diameter of 50 μm fabricated on a glass coverslip. (**a-2**) The focusing images of the protein micro-KPL in **a-1** in air under illumination with white light from a halogen lamp. The focal length is measured to be ~354 μm. (**a-3**) Optical microscope characterization of the imaging of the protein micro-KPL in **a-1**. (**a-4**) The focusing and shaping of a 532-nm-laser beam by the protein micro-KPL with a diameter of 100 μm when immersed in Rhodamine B aqueous solution. (**b-1**) The minus chromatic dispersion of a protein micro-KPL in air. The schematic shows that the white light is dispersed along the optical axis. (**b-2**–**b-6**) The optical microscope images of the focal spots of several monochromatic lights contained in the white incident light, caught at different locations on the optical axis under white light illumination. Scale bar=20 μm. (**c**) The focal lengths under illumination of monochromatic lights with different wavelengths and the corresponding curve of the protein micro-KPL in **a-1**. micro-KPL, microscale kinoform phase-type lens.

Light: Science & Applications

femtosecond laser beam (titanium-sapphire laser, Spectra Physics 3960-X1BB, 80 MHz repetition rate, 120 fs pulse width, 800 nm central wavelength) was tightly focused in the ink by a high-numerical aperture (NA=1.35) oil-immersion objective (60×). Because the two-photon-induced polymerization of the BSA molecules was confined to the core region of the laser focal spot, high laser energy density over the threshold of the two-photon absorption can guarantee nanoscale precision for the BSA hydrogel microstructures (with ⩽200 nm minimum line width here.[27]) To achieve three-dimensional (3D) microstructures, a piezo stage with 1-nm precision (PI P-622 ZCD) was used to control the sample's vertical movements. Simultaneously, the beam's horizontal scanning was performed by a two-galvano-mirror set. The complicated 3D geometry of the hydrogel microstructures was first designed in 3ds Max and then converted to computer processing data to control the 3D scanning. After the laser fabrication and water-rinsing steps, the as-formed protein micro-KPLs can be obtained on the matrix (see Figure 1a and Scheme S1 in Supplementary Information).

Because the excellent surface quality and 3D geometry quality are the prerequisites for the optical properties of protein micro-KPLs, the processing parameters have to be carefully optimized.[33] Here, a high concentration of BSA in the ink (600 mg mL^{-1}) was utilized to obtain a high crosslinking density inside protein hydrogels, which helps achieve excellent optical and mechanical properties. In fact, numerous FsLDW parameters, including the scanning step, laser power density, and exposure time on a single point, play important roles in determining the quality of the 3D geometry and the quality of the surface of the protein hydrogel microstructures, as shown in Figure 1b, and, furthermore, the final properties of the protein micro-KPLs. Herein, the exposure time on a single point was fixed at 1000 μs. When the scanning step is 100 nm or 150 nm, the laser power density should be about 48–50 mW μm^{-2}. In our work, to achieve rapidly direct writing, a scanning step of 200 nm and a laser power density of ~60 mW μm^{-2} were applied (Figure 1b). The optimal processing parameters were chosen based on the comprehensive quality of the protein microstructures shown in Figure 1b (considering the quality of both the surface and 3D geometry). As a result, the protein micro-KPLs with diameters of 50 μm, 60 μm and 80 μm could be completed with high quality in several minutes (Figure 1c-1–1c-3). The surface roughness of the protein micro-KPLs in air was approximately 10 nm, which was demonstrated by atomic force microscope (AFM), as shown in Figure 1c-4. Figure 1c-5 shows the cross section at the central line of the protein micro-KPL shown in Figure 1c-4 by AFM and shows that the 3D controllability of FsLDW is good. Such smooth surface morphology together with well-tailored 3D geometry can ensure high optical performances.

Here, the optical performances of the BSA micro-KPLs were evaluated by an upright optical microscope (Motic BA400). The pictures of imaging, focusing and chromatic dispersion were taken by properly tuning the positions of the samples along the light axis. A halogen lamp provided white light illumination, and monochromatic incident lights with different wavelengths were obtained by filtering white light with narrow-band filters (20-nm bandwidth and central wavelengths of 450 nm, 578.4 nm, 492 nm, 618.8 nm, 549 nm and 659 nm). The scanning electron microscopy (SEM) characterization was carried out using a field emission scanning electron microscope (JSM-7500F; JEOL, JEOL Ltd., Tokyo, Japan), and the samples were sputter-coated with Au film with a thickness of ~10 nm (at a current of 20 mA for 60 s) using an auto fine coater (JFC-1600; JEOL). The high BSA concentration (up to 600 mg mL^{-1}) in the processing ink and the carefully optimized FsLDW parameters resulted in a high crosslinking degree and sufficient solidity of the protein microhydrogels. Therefore, a secondary crosslinking by chemical methods, which has often been used in previous reports of protein FsLDW, was not needed.[34] Thus, protein microhydrogels were analyzed by SEM immediately after drying in the air to faithfully characterize the BSA microhydrogels in different experiment procedures (Figures 1 and 3 and Supplementary Fig. S1).

RESULTS AND DISCUSSION

Optical characteristics of protein micro-KPLs

The focusing and imaging performance of protein micro-KPLs were investigated by optical microscopy. As shown in Figure 2a, the distinct diffractive rings of micro-KPLs were apparent under illumination with white light from a halogen lamp. Using a protein micro-KPL with a size of 100 μm, a 532-nm-laser beam can be efficiently focused and shaped. To demonstrate the focusing and shaping performance of the laser, the protein micro-KPL was immersed in Rhodamine B aqueous solution; then, the laser beam was directed through the micro-KPL into the solution. By 532-nm excitation under an fluorescence microscope, the focused and shaped laser beam can easily be distinguished in the fluorescence image (Figure 2a-4). However, the incident light of the longer wavelength is more significantly bent, and the focal length is smaller, according to $f \sim 1/\lambda$. As shown in Figure 2b-1, when a beam of white light was passing through a protein micro-KPL, the monochromatic light with a longer wavelength was focused more tightly with a smaller focal length, which is the so-called 'minus chromatic dispersion' behavior. More details are shown in Figure 2b-2 through Figure 2b-6, which present optical images of the focal spots of monochromatic lights with different wavelengths at different locations along the optical axis upon white-light illumination. By plotting the measured focal lengths with the wavelengths of monochromatic incident lights, the typical minus chromatic dispersion effect is shown in Figure 2c. The focal length decreased from ~442 μm to ~311 μm by tuning the wavelength from 450 nm to 659 nm.

pH-independent optical properties of protein micro-KPLs

As reported earlier,[26,27] protein micro-hydrogels are sensitive to the pH value of surroundings. When the pH value is higher or lower than its pI (pI is the pH value under which the protein molecules are electrically neutral), the protein hydrogel will swell due to the repulsion interaction between the deprotonated carboxylate or amine group under different pH values. In our previous results, the pH effect played a significant role in the optical properties of the protein micro-optics, i.e., the protein spherical microlenses and harmonic diffractive relief microlenses. The focal length of protein microlenses can be easily adjusted by changing the pH value. However, such a pH effect is not always desirable for the application of protein micro-optics. In some cases, pH independence is required. Therefore, how to suppress the effects of pH-induced swelling or shrinking on optical properties of protein micro-optics is an open question.

It was found that the pH-induced swelling and shrinking effects can be weakened by increasing the crosslinking degree of the protein hydrogel.[34] In our work, using a high concentration of BSA solution (600 mg mL^{-1}) and optimizing the processing parameters, the crosslinking degree of the protein hydrogel could be increased. Consequently, the degree of swelling was reduced to some extent, which would be helpful for suppressing the pH response. More importantly, the structure of the micro-optics has to be designed to prevent the pH effect. For example, the focal length for protein micro-KPLs is determined by $f \approx r_m^2/m\lambda$, which means that r_m and λ are two crucial factors in determining f. However, both parameters are pH-independent. Although the swelling and shrinking effects may still occur in the

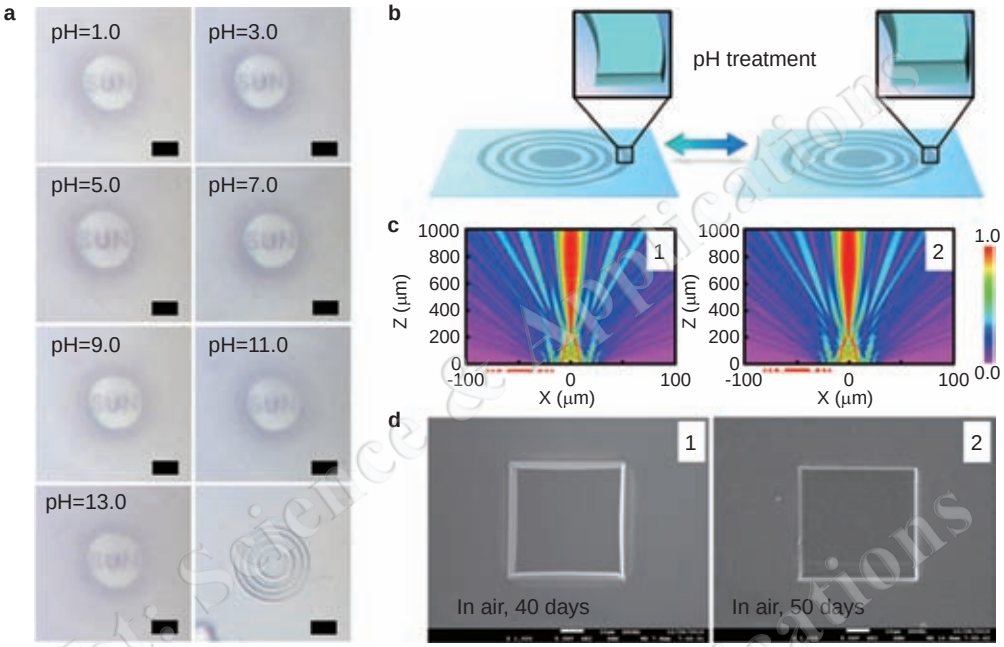

Figure 3 (**a**) Stable imaging and focusing feature of the protein micro-KPL on a glass coverslip in buffers with different values of pH. The topography of the protein micro-KPL after pH treatment is the same as the original one. Scale bar=20 μm. (**b**) The pH effect on morphology of a protein micro-KPL. The thickness, rather than the width, is changed owing to the restriction of the matrix. (**c**) Rsoft simulations of the focusing of a protein micro-KPL with a diameter of 60 μm under neutral (1) and basic or acid buffers (2). The color scale bar represents the normalized light intensity (energy). (**d**) SEM images of BSA microsquares on a glass coverslip after long-term storage in air (40 days and 50 days). BSA, bovine serum albumin; micro-KPL, microscale kinoform phase-type lens; SEM, scanning electron microscopy.

protein micro-KPL, the pH effect can change the thickness of the protein zones but not r_m, which is mainly due to the restriction of the substrates. Therefore, the r_m of a protein micro-KPL always remains constant during pH treatment (Figure 3a). Thus, the unique structure of micro-KPLs can prominently block the pH effect. These assumptions are consistent with the experimental results. As shown in Figure 3a, the protein micro-KPLs exhibit similar optical features and imaging results within a wide pH variation, from 1.0 to 13.0. During repeated pH treatment, the focused imaging did not change much. Such pH-independent behaviors can also be theoretically demonstrated by the Rsoft simulation. In Figure 3c, a protein micro-KPL with a diameter of ~60 μm was chosen for the simulation. The light energy dispersion of a protein micro-KPL to 550 nm light was calculated under different pH values, e.g., pH=7.0 (Figure 3c-1) and 13.0 or 1.0 (Figure 3c-2). For both cases, the refractive index of the buffer (n_{buffer}) was almost constant (~1.33), as measured by the Abbe refractometer. The refractive index of the BSA hydrogel (n_{hydrogel}) was obtained from our previous work.[26,27] In the case of pH=7.0, h (the micro-KPL's thickness)=1 μm, n_{hydrogel}=1.5 and n_{buffer}=1.33 (Figure 3c-1). In addition, in the case of pH= 13.0 or 1.0, h=2 μm, n_{hydrogel}=1.43 and n_{buffer}=1.33 (Figure 3c-2). The simulation results are shown in Figure 3. The two light energy dispersion simulations, as shown in Figure 3c-1 and 3c-2, were almost the same for different pHs and a moderately changing thickness of the micro-KPLs, which indicates that the optical properties of the protein micro-KPLs are relatively stable against a strong acid or base and a large pH change.

Long-term stability and biodegradability of protein micro-KPLs

The long-term stability of protein microstructures in air was demonstrated by SEM. As shown in Figure 3d, after incubation in air for 40 days, 50 days or even longer, the smooth surface and the 3D geometry of the protein microstructures did not change at all, indicating that these micro-devices have long-term stability of original topography and performances in air. In addition, similar behaviors of the protein microstructures can be observed in pure water. Obviously, the long-term stability in common operation environments greatly assists the practical application of the protein-based micro-optics.

The biodegradability of the protein microhydrogels was also investigated by SEM. After immersing them in rainwater (which contains various bacteria) under room temperature (~22 ℃) for a week, it could be observed that many bacteria grew and adhered to the surface of the protein microstructures, as shown in Figure 4b and 4e. The enlarged view in Figure 4e exhibited obvious degradation phenomena. The original smooth surface of the microstructures was obviously

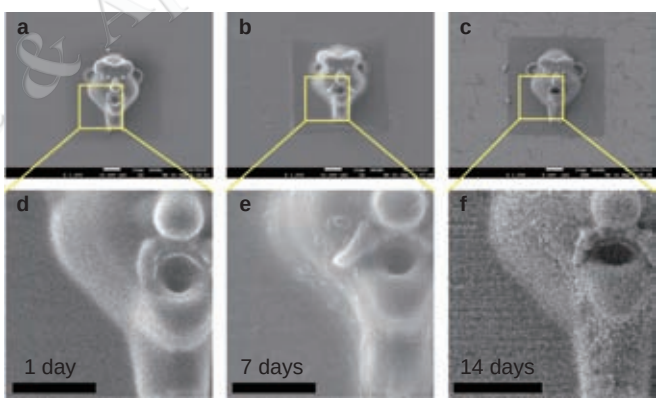

Figure 4 Biodegradation of BSA microhydrogels on a glass coverslip in rainwater at room temperature (~22 ℃). (**a**–**c**) SEM images of the BSA microhydrogel in rainwater at ~22 ℃ for 1 day, 7 days and 14 days, respectively. (**d**–**f**) SEM images of partially enlarged details of **a**–**c**, respectively. Scale bar=10 μm. BSA, bovine serum albumin; SEM, scanning electron microscopy.

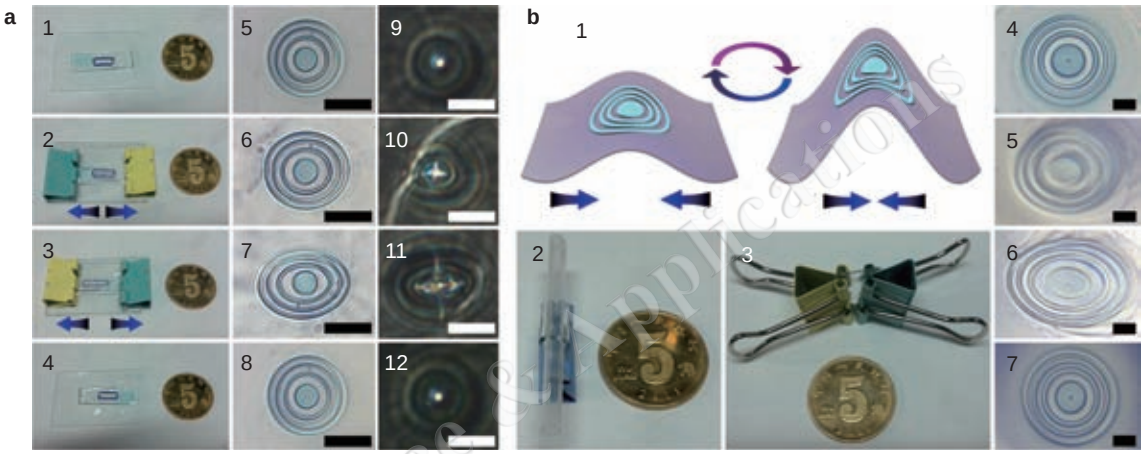

Figure 5 Flexibility of the BSA micro-KPL fabricated on a PDMS slice as the matrix. (**a**) Exhibition of the stretching ability of the BSA micro-KPL on a PDMS matrix. Scale bar=50 μm. (**b**) Exhibition of the bending ability of the BSA micro-KPL on a PDMS matrix. Scale bar=20 μm. The diameter of the coin is 20.5 mm. BSA, bovine serum albumin; micro-KPL, microscale kinoform phase-type lens; PDMS, polydimethylsiloxane.

damaged and vanished after 2 weeks (Figure 4c and 4f), and the microstructures could totally biodegrade, collapse and even disappear after several months. The biodegradation happened in an aqueous surrounding with microorganisms that cause decomposition, which indicated that the biodegradable behavior could be controllably triggered by proper external environmental conditions. These results confirmed that the protein-based micro-hydrogels fabricated by FsLDW can also be utilized as biodegradable micro-devices.

Flexibility and stretchability of protein micro-KPLs

As previously shown, the protein microhydrogels have a soft nature because their Young modulus is as low as ~4 MPa.[33] The protein microhydrogels are so soft that they can be used for flexible and stretchable optics/photonics if incorporated with suitable soft matrixes. For this reason, flexible PDMS slices were used as the matrixes where the protein micro-KPLs can be constructed by FsLDW. Then, the as-formed protein micro-KPLs on PDMS substrates exhibited interesting flexibility. First, the stretchability of the protein micro-KPLs was demonstrated by applying an external drawing force. The exhibition of the original shape of the sample, the microscopy image and the focusing test of a protein micro-KPL with a diameter of 80 μm are shown in Figure 5a-1, 5a-5 and 5a-9, respectively. By stretching, the length of the sample was increased to ~90 μm, which was approximately 1.1 times longer than the original (Figure 5a-2 and 5a-6). Then, the sample could be stretched to ~101 μm, or even larger (Figure 5a-3 and 5a-7). During the stretching process, the focal spot of the sample was deformed along with the transformation, as demonstrated in Figure 5a-9–5a-11. Once releasing the applied stress, the sample would immediately recover to the original state (Figure 5a-4), and the focusing performance was not damaged at all (Figure 5a-12). However, the bending flexibility of the sample was tested according to the method shown in Figure 5b-1. The sample was first bent and then adhered to a circular tube with a diameter of ~5 mm (Figure 5b-2). Due to the support of the curved surface, the size of the sample was elongated to ~1.2 times longer than the original length (Figure 5b-5). Furthermore, the PDMS slice with protein micro-KPLs was directly folded (Figure 5b-3), and the micro-KPL's size was increased to ~1.4 times longer than the original length (Figure 5b-6). Clear focusing images of the bent micro-KPL were difficult to obtain because different parts were not on the same plane and some were beyond the focus due to bending (Figure 5b-5 and 5b-6). Once the external bending force was removed, the initial state could rapidly be recovered, without any changes in topography or optical performances (Figure 5b-7).

CONCLUSIONS

In summary, a novel soft and biodegradable protein micro-KPL has been fabricated on PDMS matrixes by a home-made FsLDW system. Three key points are achieved in this work simultaneously. First, excellent processing quality and optical performances for practical applications are achieved. Due to the excellent surface quality and 3D geometry, the protein micro-KPLs exhibited ideal and distinctive optical properties, including the minus chromatic aberration profile, higher efficiency than the Fresnel zone plate and good imaging and focusing features. Second, the soft property of protein microhydrogels was utilized to obtain soft protein microelements for increasingly important flexible microsystems. As-formed protein micro-KPLs have excellent flexibility and stretchability, and their optical properties were not damaged after repeated stretching or bending (up to ~40% length change, or even greater by stretching or bending). Third, the valuable balance between the biodegradation in natural aqueous environments and sufficient stability in common operation environments, required for the utilization of protein micro-KPL as an environment-friendly and practical micro-optical element, was maintained. For example, in rainwater with a variety of microorganisms, preliminary but obvious biodegradation occurred after ~14 days, but in pure water and air, the sample was unchanged after more than 50 days. In contrast to the previously reported protein microlenses, the optical properties of the protein micro-KPLs were hardly influenced by pH value (from 1.0 to 13.0) due to their optical features, which ensure that they would work properly in relatively harsh conditions (e.g., in strong acid or base) and in occasions with no need for stimuli-response. The organic combination of the three points by the FsLDW approach led to the realization of protein-based 'green' soft micro-optics with diverse merits such as being biocompatible and environmentally friendly. Such soft protein micro-optics would have great potential in applications such as flexible and stretchable photonics and optics as well as soft integrated optical microsystems.

ACKNOWLEDGEMENTS

HBS thanks the National Science Foundation of China (Grant No. 90923037) and the National Basic Research Program of China (973 Program) (Grant No. 2011CB013005) for support. WFD thanks the National Science Foundation of

China (Grant Nos. 91123029, 61077066, 61137001 and 61127010) and the 863 Project of China (Grant No. 2012AA063302) for financial support.

1 Dong L, Agarwal AK, Beebe DJ, Jiang HR. Adaptive liquid microlenses activated by stimuli-responsive hydrogels. *Nature* 2006; **442**: 551–554.
2 Rogers JA, Bao ZN, Baldwin K, Dodabalapur A, Crone B *et al*. Paper-like electronic displays: large-area rubber-stamped plastic sheets of electronics and microencapsulated electrophoretic inks. *Proc Natl Acad Sci USA* 2001; **98**: 4835–4840.
3 Sirringhaus H, Tessler N, Friend RH. Integrated optoelectronic devices based on conjugated polymers. *Science* 1998; **280**: 1741–1744.
4 Kim JY, Lee K, Coates NE, Moses D, Nguyen TQ *et al*. Efficient tandem polymer solar cells fabricated by all-solution processing. *Science* 2007; **317**: 222–225.
5 Shrotriya V. Polymer power. *Nat Photonics* 2009; **3**: 447–449.
6 Taylor RA, Otanicar T, Rosengarten G. Nanofluid-based optical filter optimization for PV/T systems. *Light Sci Appl* 2012; **1**: e34; doi:10.1038/lsa.2012.34.
7 Monat C, Domachuk P, Eggleton BJ. Integrated optofluidics: a new river of light. *Nat Photonics* 2007; **1**: 106–114.
8 Dai D, Bauters J, Bowers JE. Passive technologies for future large-scale photonic integrated circuits on silicon: polarization handling, light non-reciprocity and loss reduction. *Light Sci Appl* 2012; **1**: e1; doi:10.1038/lsa.2012.1.
9 Hwang SW, Tao H, Kim DH, Cheng HY, Song JK *et al*. A physically transient form of silicon electronics. *Science* 2012; **337**: 1640–1644.
10 Mannoor MS, Tao H, Clayton JD, Sengupta A, Kaplan DL *et al*. Graphene-based wireless bacteria detection on tooth enamel. *Nat Commun* 2012; **3**: 763.
11 Kim RH, Tao H, Kim TI, Zhang YH, Kim S *et al*. Materials and designs for wirelessly powered implantable light-emitting systems. *Small* 2012; **8**: 2812–2818.
12 Kim S, Mitropoulos AN, Spitzberg JD, Tao H, Kaplan DL *et al*. Silk inverse opals. *Nat Photonics* 2012; **6**: 818–823.
13 Parker ST, Domachuk P, Amsden J, Bressner J, Lewis JA *et al*. Biocompatible silk printed optical waveguides. *Adv Mater* 2009; **21**: 2411–2415.
14 Amsden JJ, Domachuk P, Gopinath A, White RD, Negro LD *et al*. Rapid nanoimprinting of silk fibroin films for biophotonic applications. *Adv Mater* 2010; **22**: 1746–1749.
15 Lawrence BD, Cronin-Golomb M, Georgakoudi I, Kaplan DL, Omenetto FG. Bioactive silk protein biomaterial systems for optical devices. *Biomacromolecules* 2008; **9**: 1214–1220.
16 Lin DM, Tao H, Trevino J, Mondia JP, Kaplan DL *et al*. Direct transfer of subwavelength plasmonic nanostructures on bioactive silk films. *Adv Mater* 2012; **24**: 6088–6093.
17 Kim RM, Lu NS, Ma R, Kim YS, Kim RH *et al*. Epidermal electronics. *Science* 2011; **333**: 838–843.
18 John G, Jadhav SR, Menon VM, John VT. Flexible optics: recent developments in molecular gels. *Angew Chem Int Ed* 2012; **51**: 1760–1762.
19 Vidyasagar A, Handore K, Sureshan KM. Soft optical devices from self-healing gels formed by oil and sugar-based organogelators. *Angew Chem Int Ed* 2011; **50**: 8021–8024.
20 Ghosh S, Reddy CM. Elastic and bendable caffeine cocrystals: implications for the design of flexible organic materials. *Angew Chem Int Ed* 2012; **51**: 10319–10323.
21 LaFratta CN, Fourkas JT, Baldacchini T, Farrer RA. Multiphoton fabrication. *Angew Chem Int Ed* 2007; **46**: 6238–6258.
22 Kawata S, Sun HB, Tanaka T, Takada K. Finer features for functional microdevice. *Nature* 2001; **412**: 697–698.
23 Xiong W, Zhou YS, He XN, Gao Y, Mahjouri-Samanil M *et al*. Simultaneous additive and subtractive three-dimensional nanofabrication using integrated two-photon polymerization and multiphoton ablation. *Light Sci Appl* 2012; **1**: e6; doi:10.1038/lsa.2012.6.
24 Zhang YL, Chen QD, Xia H, Sun HB. Designable 3D nanofabrication by femtosecond laser direct writing. *Nano Today* 2010; **5**: 435–448.
25 Basu S, Wolgemuth CW, Campagnola PJ. Enzymatic activity of alkaline phosphatase inside protein and polymer structures fabricated *via* multiphoton excitation. *Biomacromolecules* 2004; **5**: 2347–2357.
26 Sun YL, Dong WF, Yang RZ, Meng X, Zhang L *et al*. Dynamically tunable protein microlenses. *Angew Chem Int Ed* 2012; **124**: 1590–1594.
27 Sun YL, Liu DX, Dong WF, Chen QD, Sun HB. Tunable protein harmonic diffractive micro-optical elements. *Opt Lett* 2012; **37**: 2973–2975.
28 Kaehr B, Allen R, Javier DJ, Currie J, Shear JB. Guiding neuronal development with *in situ* microfabrication. *Proc Natl Acad Sci USA* 2004; **101**: 16104–16108.
29 Cho KC, Lien CH, Lin CY, Chang CY, Huang LL *et al*. Enhanced two-photon excited fluorescence in three-dimensionally crosslinked bovine serum albumin microstructures. *Opt Express* 2011; **19**: 11732–11739.
30 Lin CY, Lien CH, Cho KC, Chang CY, Chang NS *et al*. Investigation of two-photon excited fluorescence increment *via* crosslinked bovine serum albumin. *Opt Express* 2012; **20**: 13669–13676.
31 Pitts JD, Campagnola PJ, Epling GA, Goodman SL. Submicron multiphoton free-form fabrication of proteins and polymers: studies of reaction efficiencies and applications in sustained release. *Macromolecules* 2000; **33**: 1514–1523.
32 Chen QD, Wu D, Niu LG, Wang J, Lin XF *et al*. Phase lenses and mirrors created by laser micronanofabrication *via* two-photon photopolymerization. *Appl Phys Lett* 2007; **91**: 171105.
33 Khripin CY, Brinker CJ, Kaehr B. Mechanically tunable multiphoton fabricated protein hydrogels investigated using atomic force microscopy. *Soft Matter* 2010; **6**: 2842–2848.
34 Kaehr B, Shear JB. Multiphoton fabrication of chemically responsive protein hydrogels for microactuation. *Proc Natl Acad Sci USA*. 2008; **105**: 8850–8854.

This work is licensed under a Creative Commons Attribution-NonCommercial-ShareAlike 3.0 Unported license. To view a copy of this license, visit http://creativecommons.org/licenses/by-nc-sa/3.0

Supplementary information for this article can be found on the *Light: Science & Applications*' website (http://www.nature.com/lsa/).

Light: Science & Applications